A Quantum-Classical Hybrid Branch & Bound Algorithm

András Czégel 1* , Dávid Sipos 2 and Boglárka G.-Tóth 1

- ^{1*}Department of Computational Optimization, University of Szeged, Árpád tér 2., Szeged, 6720, Hungary.
- ^{2*}Institute for Algorithms and Complexity, TU Hamburg, Hamburg, 21079, Germany.

Abstract

We propose a complete quantum-classical hybrid branch-and-bound algorithm (QCBB) to solve binary linear programs with equality constraints. That includes bound calculation, convergence metrics and optimality guarantee to the quantum optimization based algorithm, which makes our method directly comparable to classical methods. Key aspects of the proposed algorithm are (i) encapsulation of the quantum optimization method, (ii) utilization of noisy samples for problem reduction, (iii) classical approximation based bound calculation, (iv) branch and bound traits like gap-based stopping criterion and monotonic increase in solution quality, (v) integrated composition of many different solutions that can be improved individually. We show numerical results on set partitioning problem instances and provide many details about the characteristics of the different steps of the algorithm.

1 Introduction

Quantum optimization is one of the most rapidly advancing fields of quantum technology. It has been in the headlines because the many promises over classical algorithms on certain problems. A comprehensive article recently investigated the different approaches and their challenges [1]. When we look for solutions to Integer Linear Programming (ILP) problems, most quantum optimization algorithms, like Quantum Approximate Optimization Algorithm (QAOA) family [2–4], the variational Quantum Imaginary Time Evolution (varQITE) algorithm [5–7] and the Quantum Iterative Power Algorithms (QIPA) [8] are designed to tackle the whole problem at once, even

though, utilizing different principles. Classical optimization solvers are usually composed of many different algorithms [9–15] to solve carefully constructed subproblems. Our aim is to adapt this approach to quantum optimization solutions as well.

To provide context for our hybrid approach, we take a brief look at the literature, investigating ideas related to decomposition-based and sequential hybrid optimization.

There has been a recursive decomposition scheme introduced to QAOA by Bravyi et al. in [16, 17]. In their algorithm, RQAOA, correlations are computed in the physical system, and then system size is reduced with the aim of breaking symmetries, leading to improvement over the original QAOA algorithm. A new algorithm family, Quantum-Informed Recursive Optimization Algorithms (QIRO) [18], goes further on this path: they enhanced decomposition steps by classical, problem dependent rules and backtracking. Computing correlations can suffer from noise and algorithmic error of the QAOA, leading to wrong decisions when reducing the systems. To some extent, the backtracking in QIRO resolves this issue, however, it does not build a complete tree during recursive simplifications, thus it does not guarantee to find optimal solutions. There is also a promising recent work on how deep learning can enhance the performance of variational quantum optimizers [19], although the algorithm does not guarantee optimality either.

While these algorithms apply a recursive decomposition, another idea of enhancing variational quantum optimization algorithms is by classically computing warmstart values to the variational parameters [20], which also leads to significant improvements over the original variational quantum algorithm.

The other side of finding new hybrid optimization solutions is by classical techniques from Operations Research. These are powerful tools, even though they do not enhance the quantum optimization routine itself, but utilize it better. One such approach is to use Benders decomposition to split the mixed ILP problem to a continuous linear program and a quadratic unconstrained binary problem designed to solve on quantum computers [21]. There were also studies towards a quantum branch and bound algorithm [22, 23] by using quantum tree search [24] and estimating the tree size [25], resulting in a near-quadratic speedup on the tree search. This algorithm, even though belongs to the same family of algorithms, uses a vastly different approach from our branch and bound construction in each of its main steps.

We have also proposed a conflict-driven constraint generation algorithm for binary linear programs [26]. In that idea, the quantum algorithm is used to solve an unconstrained relaxation of the original problem, and then iteratively adding back constraints until the quantum algorithm successfully finds high-quality feasible solutions.

In this work, we take a step further along this path of wrapping an arbitrary variational quantum optimization algorithm. We propose a conflict-driven branch and bound method that has a decomposition structure with bounds and guarantees. We solve each subproblem with a quantum device that provide solution candidates by sampling its solutions state. From those samples, we derive a quantity for each variable, which tells us of how much complication it holds, i.e. how many conflicting constraints it is involved in. We call them conflict values, and we use them to select branching variables. We also use constraint propagation to further reduce problem size at each branching step. With combining these techniques, we aim to reduce the complexity

and the size of the problem at each step, driving the quantum algorithm towards better quality solutions. We also designed a fast classical bounding method, that enables us to cut the branch and bound tree, and more importantly, to prove optimality.

With this work we would like to provide a ground for further advancements. Our work does not aim to top classical solutions on industrially relevant problems, but a proof of concept. We provide a framework that can be highly improved by optimizing its parts for the respective problem, software and hardware requirements.

Our paper is structured as follows: first we introduce the problem in Section 2, then describe the QCBB algorithm in Section 3. After that we provide numerical results in Section 4. Then, we discuss how the algorithm behaves, discuss improvement opportunities and provide more contextual information in Section 5.

2 Problem

Our initial, master problem (MP) is to find a solution to a binary linear problem,

min
$$\{c^T x \mid Ax = b, x \in \{0,1\}^n\},$$
 (MP)

where $c \in \mathbb{R}^n$, $A \in \mathbb{R}^{m \times n}$, $b \in \mathbb{R}^m$. This can be generalized to integer variables [27, 28]. In the following sections we propose an algorithm to solve (MP).

2.1 Master Hamiltonian

We transform (MP) into an Ising Hamiltonian. For this transformation, we create a Quadratic Unconstrained Binary Optimization (QUBO) form of it, and then transform variables from the $\{0,1\}$ domain to the $\{-1,1\}$ domain. The transformation is derived in Appendix A.1. The Ising Hamiltonian, which we name as Master Hamiltonian (MH) for future reference, is the following:

$$H(\sigma) = -\sum_{i < j} J_{ij}\sigma_i\sigma_j - \mu \sum_i h_i\sigma_i, \tag{MH}$$

where

$$J = -\frac{1}{4}MA^{T}A\tag{1}$$

and

$$h = c^T - 2Mb^T A + M\mathbf{1}^T (A^T A) \tag{2}$$

with

$$\mu = -\frac{1}{2},\tag{3}$$

where big M is a sufficiently large constant, and by putting aside a constant term

$$C = \frac{1}{4}M\mathbf{1}^{T}(A^{T}A)\mathbf{1} + \frac{1}{2}\mathbf{1}^{T}c - Mb^{T}A\mathbf{1} + Mb^{T}b$$
(4)

from the objective function. One can find exact calculations for big M in [26] and in Appendix A.2.

3 Quantum-Classical Branch & Bound

Our proposal is an algorithm that uses quantum computing within a branch-and-bound framework. The branch-and-bound is a general optimization framework that searches for the best solution through recursive decomposition of the problem into smaller subproblems (branching). For each subproblem, bounds on the objective value are computed to estimate its potential. Subproblems whose bounds indicate no improvement over the current best solution are discarded (pruned). This recursive branching, bounding, and pruning process continues until all promising regions are explored, thus the global optimum is found without the complete enumeration of all possible solutions.

The algorithm builds a decomposition tree. Note that this is a recursive definition for building an evaluation tree, where in this case the root is the master problem, and subproblems get simpler and smaller along the path to leaf nodes. From now on, let us denote the elements of the problem of the node under evaluation by $\hat{H}, \hat{A}, \hat{b}, \hat{c}, \hat{x}, \hat{\sigma}$ having \hat{n} variables, corresponding to (MH)-(4) for the reduced problem

min
$$\left\{ \hat{c}^T \hat{x} \mid \hat{A} \hat{x} = \hat{b}, \ \hat{x} \in \{0, 1\}^{\hat{n}} \right\}$$
. (RP)

We denote child node subproblem elements by tilde on the respective element. At any point of time of the execution, the feasible set of the subproblems in the frontier of the tree contains the optimal solution of the problem at the root, the master problem.

In general, the definition of a branch-and-bound framework requires the specification of the following rules: branching, node selection, bounding, pruning and termination. Quantum computation is involved in the branching and bounding rules; therefore, we will focus on describing them first.

3.1 Variational Quantum Solution

At this point, (MH) encodes our feasible solutions in its lower energy states. Now we look for a suitable VQA to search for these states. Here we chose the QAOA for simplicity and clarity, but any VQA suffices.

Our aim is to find the state preparation routine U such that $U|0\rangle^{\otimes n} = |\psi^*\rangle$, where $|\psi^*\rangle$ corresponds for the ground state of the Hamiltonian ideally. In reality, $|\psi^*\rangle$ is rather a superposition of states that we hope to belong to low energy levels, i.e. encode feasible solutions to (MP). Upon measurement, we get a sample from a probability distribution that the measurement represents with respect to the state.

We can use this behavior to sample from the result state q times to look for good solutions, and also for other information that we can utilize. We denote the number of different samples by s and their respective counts in the samples by $\omega = (\omega_1, \ldots, \omega_s)$

where
$$\sum_{i=1}^{s} \omega_i = q$$
.

Let us denote the gathered different samples by X, where sample ℓ is the ℓ th column of X, i.e. where $X_{i\ell}$ is x_i of sample ℓ , for $\ell = 1, \ldots, s, \ i = 1, \ldots, n$.

Then, the solution for the problem at hand, coming from (MH), is given by the sample that has the least energy value.

3.2 Branching

Branching means that the selected subproblem is decomposed into smaller problems. Generally it can be done by selecting a branching variable and separating the problem by restricting its bounds. In order to choose the variable to branch at, we use the gathered information from the samples. If there is an improving solution among the samples, i.e. the value of it is less than the previous best, that solution becomes the incumbent.

3.2.1 Conflict values

In this step we derive conflict values for variables. This tells about a variable, that how much constraint violations it has been part of.

First, we define violation matrix $V \in \{0,1\}^{m \times s}$, where

$$V_{j\ell} = \begin{cases} 1, & \text{when } \sum_{i} \hat{A}_{ji} X_{i\ell} - \hat{b}_{j} \neq 0 \\ 0, & \text{otherwise.} \end{cases}$$
 (5)

Note that V does not represent how much these constraints were violated. Since we don't deal with numeric issues here explicitly, the aim is to reduce the number of overall violations. In other words, we don't look for extreme outliers, but for controversial variables.

We can obtain violation scores as dual-like quantities for each constraint j by

$$\nu_j = \frac{1}{q} \sum_{\ell=1}^{s} V_{j\ell} \omega_{\ell} \qquad j = 1, \dots, m.$$
 (6)

This gives a normalized vector $\nu \in [0,1]^m$, where each ν_j tells us what proportion of the samples violated constraint j of (MP). Using ν , we can derive a conflict value for each variable x_i that tells us how much it contributes to constraint violations. For that, let P denote the correspondence matrix for variables in constraints as

$$P_{ji} = \begin{cases} 1, & \text{when } \hat{A}_{ji} \neq 0 \\ 0, & \text{otherwise.} \end{cases}$$
 (7)

Then, the conflict vector $\gamma \in \mathbb{R}^{\hat{n}}$ is computed as

$$\gamma = \nu P. \tag{8}$$

In other words, γ_i measures for each variable x_i , how much it contributes to constraint violations.

Note that these conflict values in general do not depend on the actual objective coefficient of the variable they belong to. However, we can use the information of the variable values later for branch selection.

3.2.2 Variable selection

We select the most conflicting variable to branch on, i.e.

$$k = \arg\max_{i} \gamma_{i}. \tag{9}$$

Restricting variables on their bounds on binary programs also mean setting their value exactly.

3.2.3 Subproblem construction

The variable selected by (9) can be removed then from the current problem as if we set $\hat{x}_k = 0$ or $\hat{x}_k = 1$,

$$\tilde{b}_i = \hat{b}_i - \hat{A}_{ik}\hat{x}_k \qquad \forall j \tag{10}$$

To update \hat{A} and \hat{c} and remove \hat{x}_k , we define the column-elimination matrix D as an $\hat{n} \times \hat{n} - 1$ matrix, which is obtained by removing column k from the identity matrix. Now define the new coefficients of the new subproblem using

$$\tilde{A} = \hat{A}D, \qquad \tilde{c} = D^T\hat{c}, \qquad \tilde{x} = D^T\hat{x}$$
 (11)

that removes variable \hat{x}_k from (RP) and adjusts the problem structure to its fixed value.

Consequently, the Reduced Hamiltonian (RH) for the new subproblem is

$$\tilde{H}(\tilde{\sigma}) = -\sum_{i < j} \tilde{J}_{ij} \tilde{\sigma}_i \tilde{\sigma}_j - \mu \sum_j \tilde{h}_i \tilde{\sigma}_i, \tag{RH}$$

where

$$\tilde{J} = -\frac{1}{4}M\tilde{A}^T\tilde{A} \tag{12}$$

and

$$\tilde{h} = \tilde{c}^T - 2M\tilde{b}^T\tilde{A} + M\mathbf{1}^T(\tilde{A}^T\tilde{A}) \tag{13}$$

with $\mu = -\frac{1}{2}$. Note that $\tilde{\sigma} = D^T \hat{\sigma}$, eliminating the kth element of $\hat{\sigma}$. The Hamiltonian is also of size $\hat{n} - 1 \times \hat{n} - 1$, where \hat{n} denotes the size of the recently evaluated node's problem. While constructing $\tilde{H}(\tilde{\sigma})$, we get an additional constant term that we put aside during the quantum optimization step. This constant, however, is needed to obtain the solution to (MP). It is composed from the constant part of the transformation to Ising Hamiltonian,

$$\tilde{C}_{\text{transform}} = \frac{1}{4} M \mathbf{1}^T (\tilde{A}^T \tilde{A}) \mathbf{1} + \frac{1}{2} \mathbf{1}^T \tilde{c} - M \tilde{b}^T \tilde{A} \mathbf{1} + M \tilde{b}^T \tilde{b}, \tag{14}$$

and from the part that comes from the objective coefficient of the eliminated variable,

$$\tilde{C}_{\text{objective}} = \hat{C}_{\text{objective}} + \hat{c}_k \hat{x}_k,$$
 (15)

thus the constant term is

$$\tilde{C} = \tilde{C}_{\text{transform}} + \tilde{C}_{\text{objective}}.$$
 (16)

3.2.4 Variable bound propagation

In binary problems, branching on a variable is not just a restriction, but an exact assignment. By assigning 0 or 1 to a variable, there might be other enforced reductions in the problem. These reductions come from dependence on the assigned variable in other constraints. On the other hand, either the original or the propagated reductions could discover infeasibility, which allow us to prune the whole sub-tree. This direction of reduction is well described in [18] and used as propagation logic inside SAT-solvers that are based on the Davis–Putnam–Logemann–Loveland (DPLL) algorithm [29, 30].

The propagation of some variables means that the problem becomes even smaller. These variables are treated in the same way as the branching variable, which means that we apply the formulas (10)-(16) with all fixed variables where D becomes a matrix having all columns with fixed variables removed.

The complete subproblem creation and propagation creates a tree structure, shown on Figure 1, where the process inside a node evaluation is on Figure 2.

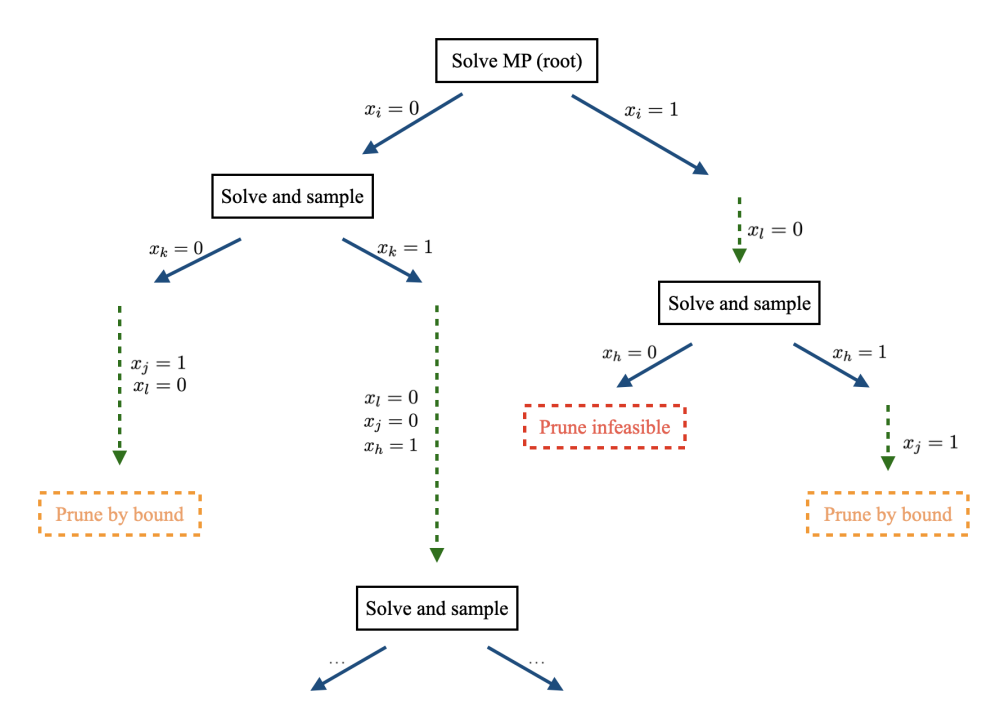


Figure 1 An example for the tree of the branching algorithm. First, the Master Problem is solved. Then, we branch by assigning values to one variable (blue arrows). After that, we try to further reduce the problem by constraint propagation steps, that also assign values to variables (green dashed arrows). In each node, we calculate a bound, and if possible, prune based on that (orange node). We also prune infeasible subproblems (red nodes).

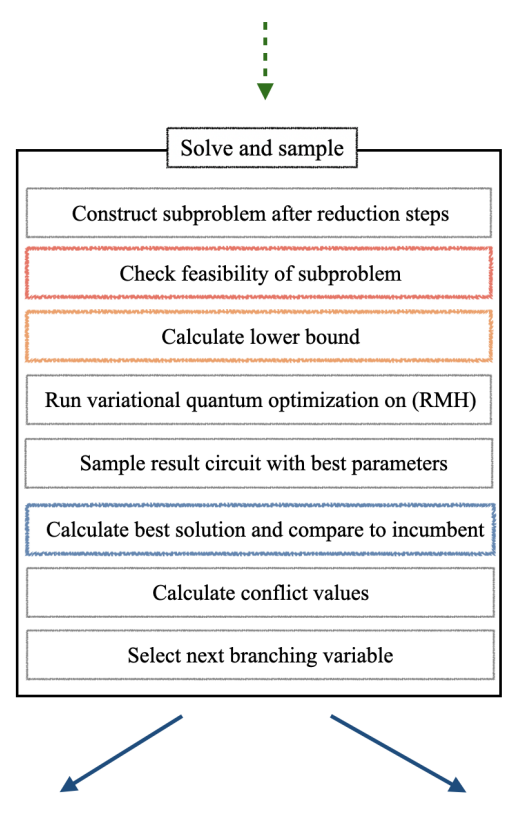


Figure 2 Steps of a single node evaluation in the tree. The boxes with thick red, orange borders note the prune criteria: checking infeasibility and bounding. The blue box indicates the possible update on the incumbent value.

3.3 Node selection

In this initial work we choose in each iteration the next node to be evaluated by the lowest lower bound. This is a simple, standard strategy that has some good aspects to it. It gives the greatest opportunity to reduce the gap between the incumbent solution value and the global lower bound. This can be viewed as a greedy selection rule, which minimizes the number of evaluated nodes, trying to close the gap with as few steps as possible. This comes handy as node evaluation is the most expensive step in our algorithm.

3.4 Bounding

Bounding is an important step for reducing the search space, and allowing effective cuts to the tree. Lacking of an LP-relaxation and thus a relaxed bound to (RP) poses a major challenge on how to get a meaningful lower bound. Here, we propose an efficient approximation-based lower bound calculation to obtain good lower bounds at each node. The strategy itself is simple, and bounds the reduced problem at the given node. Since our branching decisions are variable assignments that lead to problem

reductions, we can consider a bound on the reduced objective (RH), corrected with the constant terms to obtain a valid lower bound to the original problem. The bounding has the following three steps: (i) transform (RH) to a Maximum Cut problem, (ii) obtain approximate solution, z_{GW} , to the Maximum Cut by the Goemans-Williamson algorithm [31], and (iii) calculate bound based on the guaranteed approximation ratio.

The lower bound is obtained by

$$LB_{GW}(\hat{H}(\sigma)) = -\frac{2}{\alpha}z_{GW} + \left(\frac{2}{\alpha} - 2\right)W^{-} + W, \tag{17}$$

where $\alpha = 0.87856$, which is the average worst-case approximation ratio of the Goemans-Williamson algorithm,

$$W^{-} = \sum_{i < j, J_{ij} < 0} \hat{J}_{ij} + \mu \sum_{i: h_i < 0} \hat{h}_i, \quad \text{and} \quad W = \sum_{i < j} \hat{J}_{ij} + \mu \sum_i \hat{h}_i, \quad (18)$$

i.e. W^- is the sum of all negative coefficients in $\hat{H}(\sigma)$ and W is the sum of all coefficients in $\hat{H}(\sigma)$. If the bound is looser than the bound from the parent node, we take the bound from the parent node. Thus, for any child node problem defined by \tilde{H} and parent node problem \hat{H} , omitting the variables from the notation for convenience,

$$LB(\tilde{H}) = \max \left\{ LB_{GW}(\hat{H}), LB(\hat{H}) \right\}. \tag{19}$$

Since this only bounds the Hamiltonian's ground state energy, we need to add back the constant term (16) to get a lower bound to the node under evaluation. We discuss the calculations and quality guarantees in Appendix B. Adding back all the fixed variable values, we end up at a local lower bound for the sub-tree, rooted at the evaluated node. The lowest of these bounds in the frontier of the tree is the global lower bound, due to the disjunctive structure of the subproblems. Note that when we reach a subproblem with no free variables, $LB_{GW}(\hat{H}(\sigma)) = \hat{C}_{\text{objective}} = \sum_{k \in \{1..n\}} c_k x_k$,

which is then equal to the actual value of the objective.

3.5 Pruning

The branch-and-bound framework uses the bound calculation to prune nodes and their sub-tree. If the lower bound of the subproblem at a given node is greater than the incumbent that we got from the variational quantum algorithm, we can prune the tree at the node, because the subproblem can not provide any improvement on the incumbent.

3.5.1 Infeasibility pruning

After the branching assignment, and possible further assignments from bound propagation, we have more information about the problem that we can use. The set of assignments might reveal contradictions in the constraints. If we find such a contradiction, the subproblem is infeasible and we can prune the branch.

The individual constraint contradiction itself is sufficient to prove infeasibility, but its absence does not prove feasibility. The subproblem constraints could each be satisfied on its own, while these assignment contradict each other.

With our current bounding strategy, we can define one more feasibility based pruning rule, because if $LB_{GW}(\hat{H}) + \hat{C} \geq M$, then the subproblem is infeasible. We provide details to this in Appendix C.

Checking and proving feasibility of the subproblem itself is NP-complete [27]. Despite the lack of guarantee of feasibility, this is a good condition for pruning.

3.6 Stopping criteria

Some quantum algorithms, like the QAOA family [2–4] and other time evolution based methods [5–7] offer rigorous error measures and guarantees, however these are hard to realize on current quantum hardware [32]. While there are many ways to improve the performance and precision of the quantum optimization routine [33–36], mathematical guarantees remain difficult to achieve in a practical setting.

The flipside is, hybrid quantum optimization algorithms themselves aim to find optimal solutions to the discrete optimization problem, and not the relaxation. This provides a highly uncertain advantage: they might find good quality, or even optimal solutions early. However they could, in practice, provide infeasible solutions in all the samples of the output state. In this algorithm, we work on these nodes as well, and continue until the point where where bounds themselves provide proof of infeasibility or non-optimality. At that point the quantum algorithm can either produce feasible solutions or we can prove the infeasibility of the subproblem itself.

Coming from the scheme of branch and bound, there are some criteria based on which one could stop the run, for example (i) number of evaluated nodes, and (ii) runtime, (iii) proven optimality and (iv) duality gap target value. The first two is straightforward, measuring the number of evaluated nodes and runtime, and stop upon we reach the limit. Then, return the best solution found so far.

3.6.1 Proven optimality

Traditionally, quantum algorithms don't have lower bounds, nor strict convergence guarantees on which they can be stopped. We aim to change that. We obtain global lower bound, described in Section 3.4. When the global lower bound meets the current upper bound, the incumbent solution, we have a proof of optimality.

3.6.2 Target gap value

Of course, reaching optimality can take exponential time, and there are bound-based criteria. One of them is to calculate the ratio between the upper bound and lower bound, defining a gap value. This gap is monotonically decreasing due to the structure of branch and bound. While reaching a given gap might also take exponential time, in reality, reaching a reasonable gap is usually faster and more viable solution than going for proven optimality. With that said, stopping early still holds a valuable information: how far are we, in the worst case, from an optimal solution.

4 Results

We applied our method to many different instances of the Set Partitioning Problem (SPP). The problem has practical applications, for example in scheduling airline crews [37].

4.1 Set Partitioning Problem

In this problem, given a collection $S = \{s_1, \ldots, s_n\}$ of subsets of a set $R = \{r_1, \ldots, r_m\}$ and associated costs $C = \{c_1, \ldots, c_n\}$, we are looking for a subset $S^* \subset S$ which covers exactly once every element of R at minimum total cost.

By associating every subset s_i with a variable x_i , and defining $a_{ij} = 1$ if $r_j \in s_i$, 0 otherwise, the problem can be modeled as the following binary linear program,

$$\min \quad \sum_{i=1}^{n} c_i x_i \tag{20}$$

s.t.
$$\sum_{i=1}^{n} a_{ij} x_{i} = 1 \qquad \forall j \in \{1, \dots, m\}$$
 (21)
$$x_{i} \in \{0, 1\} \qquad \forall i \in \{1, \dots, n\}$$
 (22)

$$x_i \in \{0, 1\} \qquad \forall i \in \{1, \dots, n\} \tag{22}$$

We transform this formulation as described in Section 2.1.

4.2 System integration

We utilized the benchmark suite developed in previous work [37] to test our algorithm. The solve and sample, and branching steps, illustrated in Figure 1 and Figure 2, are implemented as a plugin in the benchmark suite, which can leverage already existing integrations of quantum computing providers, optimizers and QAOA ansätze while also being usable on its own as a Python module. Execution of the algorithm on different problems is conducted through what is referred to as an Experiment in the suite, which allows the creation and reuse of configuration files to produce and extract insights about the algorithm's behavior which we expand on in the following section.

4.3 Experimental results

Keeping in mind constrained computational resources, we tested the algorithm on randomly generated instances of SPP. For every instance, at least a single feasible solution is guaranteed and no instance contains the complete set, i.e. $s_i \subset R \ \forall i$. All problem instances have n = 15 variables (subsets) and a varied number of constraints (m elements), resulting in a quantum circuit with 15 qubits. In our testing we used the QAOA algorithm [2], at the depth of p=3, for simplicity with no platform specific circuit, or hardware optimizations as we focus on the classical framework in this work. For optimizing the expectation value of the quantum state, we use the COBYLA [38] algorithm.

For measuring branch and bound algorithms, and in general, classical mixed-integer linear programming (MILP) solvers, there is a concept called the primal-dual integral [39]. In short, it measures how the best solution (primal) and the best lower bound (dual) change over time. Since both converge to an optimal solution value, the area between them measures the quality of the solution process of a solver (the area between the red and blue lines in Figure 3). We do not solve the LP-relaxation of the binary program, but, as described in Section 3.4, we obtain a bound based on the equivalent Maximum Cut formulation of the problem. So in traditional sense we do not calculate dual problems, but a monotonic improving lower bound which qualifies the algorithm to be measured by this metric.

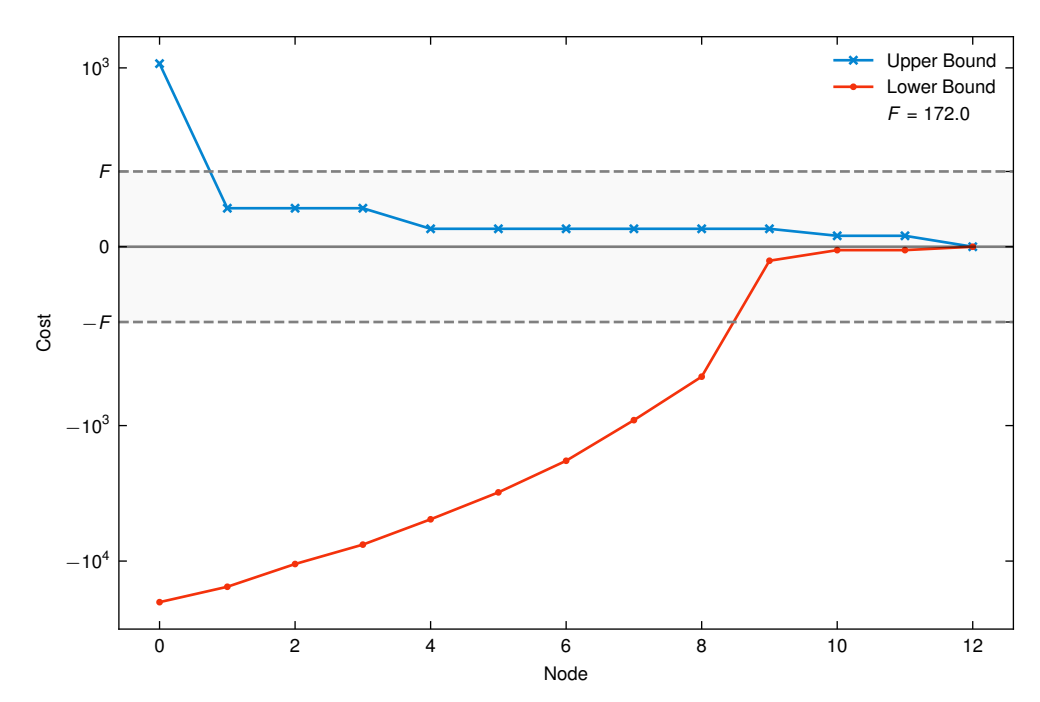


Figure 3 Convergence of bounds. A blue line with x-shaped markers shows the upper bound (cost of incumbent solution) as a function of the number of nodes evaluated. The red line with circular markers shows the lower bound as the function of the number of nodes evaluated. A solid black line marks the optimum, aligned to 0, with dashed black lines representing the cost F of the worst feasible solution, in this case 172. Between the dashed lines the y axis is scaled linearly while outside the dashed line a logarithmic scale is used.

In Figure 3, we show on a particular problem instance how the upper and lower bounds evolve as nodes get evaluated, with further instances shown in Appendix F. Bound values are adjusted such that the optimum is at 0, marked by a solid black line. As a consequence of the penalty terms introduced in the QUBO formulation, bound values associated with infeasible solutions are quite large, as such we opted to use a logarithmic scale a certain distance away from the optimum, marked by dashed black lines. This distance, F, is given by the highest-cost feasible solution, and within its distance from the optimum the scale is linear. The blue line with x-markers represents

the evolution of the upper bound. This bound is the cost of the current incumbent (though not necessarily feasible) solution obtained either as a result of sampling the quantum state resulting from the VQA execution at that node or as a result of variable fixing. The red line with circular markers represents the evolution of the lower bound. We see that both upper and lower bounds converge as the number of nodes explored increases, for this particular instance, an optimal solution was found after exploring 18 nodes. Convergence is guaranteed by design, though we provide more explanation of that in Appendix E.

As explained in Section 3.2, the subproblem in any node has at least one variable fixed (potentially more due to further reductions), which not only results in a subproblem with fewer variables, but also one with fewer many-body interactions which can greatly impact the size of the quantum circuit not only in terms of the number of qubits required, but also the number of costly two-qubit gates. We show, in figure 4, the fraction of many-body terms present, compared to (MH), as the tree is being explored as a blue line with circular markers. Since the plot does not preserve the tree structure, we can expect to see occasional increases in the fraction of terms remaining at a given node. The number of many-body terms at a node is always less than the that in the parent node, but is not overall expected to decrease monotonically as other parts of the tree with more many-body terms might be explored during the optimization process.

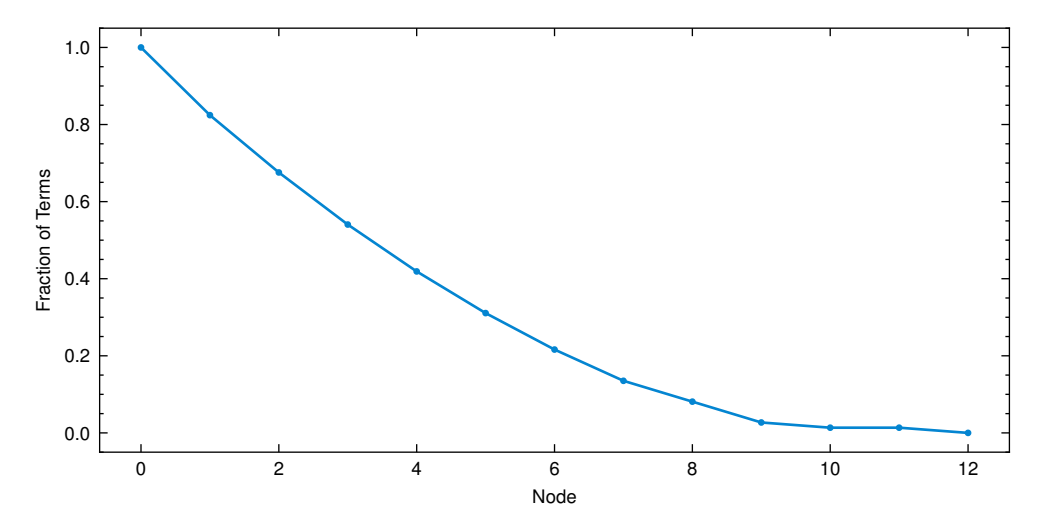


Figure 4 Fraction of many-body terms. A blue line with circular markers shows the fraction of many-body terms remaining (compared to (MH)) as a function of nodes evaluated.

To demonstrate the value of solving reduced subproblems, we can look at how our algorithm compares to just running QAOA in terms of the reducing cost associated with the quantum state reached after optimization. To compare different nodes in the tree, we must evaluate result in the context of the root node (either (MP) or (MH)), which we do by adding back constant terms arising from reductions as explained in Section 3.2.3. Since we use QAOA within our branch and bound approach, restricting

the algorithm to evaluating only a single (the root) node would be equivalent to simply relying on QAOA to solve the problem. In our experiments, we utilize the COBYLA optimizer with stricter convergence criteria, which would result in more iterations and consequently more queries being made to a quantum computer before termination of the algorithm. This is to show that splitting up these iterations over many nodes, and subproblems, is a better use of quantum computational resources than just expending a similar amount of compute on just the master problem. To this end, we configure the optimizer with a maximum number of 50 iterations per node for our branch and bound algorithm and at most 500 iterations for plain QAOA. The cost values are adjusted such that the optimum cost is 0 and the distance between the optimum and the worst feasible solution is 1.

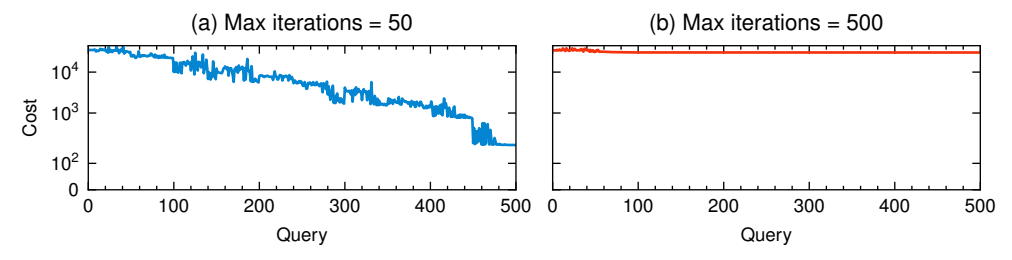


Figure 5 Comparison of branch and bound with plain QAOA. The plots show the expected cost associated with the quantum state, as a function of queries made to a quantum simulator, as it evolves during the execution of the VQA in each node. Subplot (a), in blue, uses the branch and bound approach proposed in this work with a limit of 50 iterations per node. In subfigure (b), in red, only QAOA is used. The cost at the optimum is adjusted to 0.

In our testing, we see a clear advantage attributable to the subproblem reduction step as the expected cost associated with the quantum state drops as we switch to solving smaller and smaller subproblems in Subfigure (a) of Figure 5. In contrast, with plain QAOA (Figure 5 (b)) the improvements plateau out fairly early and at higher expected cost, which can suggest a high probability of sampling suboptimal variable assignments. It is clear to see the necessity of appropriately configuring the optimizer used, so that we start branching before the improvements plateau out. Notably, the subproblem typically begins with a higher expected cost than that reached in the parent node, but tends to end up with a lower expected cost by the end of the optimization process. This opens up the question of whether parent nodes can inform the starting parametrization of child nodes.

5 Discussion

We introduced the framework for a hybrid quantum branch and bound algorithm. Since there are many parts to it, also from different fields, we aimed for simplicity and understandability. With that in mind, we would like to have a slightly more elaborate discussion section to address many different characteristic features and the possible improvements of the algorithm.

5.1 Classical algorithmic opportunities

Conflict values have a similar structure as reduced costs have in linear programming. While in linear programming, reduced costs drive towards optimality, in this algorithm conflict values drive towards feasibility. With this value, we aim then to reduce the complexity of the problem at each level of the tree as much as possible. Furthermore, this is a reduction which inherently takes differences in the chosen quantum subroutines into account. As they might find different properties of the energy land-scape harder to address, the conflict values aim to capture this hardness and resolve it by removing the right variable and branching based on its domain.

There are improvement opportunities inside the algorithm: the value of M does not change going down the tree. However, with each step, one could restrict and reduce M more and more, and consequently get problem which is numerically better, the extremes are smaller and both the VQA and the GW-bound is better. One caveat is, computing the global bound requires to compute and maintain the change of M over the nodes, for example according to [40], just like we track the change of the constant offset of H. Some of the further opportunities are improving the node selection, adding more sophisticated subproblem feasibility testing, adding proper presolving and improving the approximate bound calculation by looking at graph structure or using quadratic programming relaxations to the QUBO at hand [41, 42].

5.2 Quantum algorithmic opportunities

The algorithm has potential for further development and large improvements on the quantum side as well. One could use more sophisticated VQAs [43, 44], that could significantly enhance the overall performance as it is the heart of the algorithm. One could look for any suitable algorithm from the literature and measure their impact.

One step closer to the quantum part itself, one could find that the problem encoding we use is naive and simple. Another large improvement can be achieved by better problem encoding and use of quantum resources [45, 46].

Taking one more step, and looking into further details, one could also see that they could use more clever transpilation and compilation methods [47] and circuit optimization techniques [36]. That we also did not consider here.

5.3 Algorithm characteristics

There are also some aspects on the usability that we would like to discuss. First, while BLPs are NP-complete [27] and thus in theory any MILP can be reduced to it in polynomial time. Practically, our required problem structure is strict and tight, however reductions to it can be useful and this structure can be exploited when formulated well.

One caveat is that one needs to train a VQA at each node. In general, that is expensive and slow. However we do not rely strictly on their solution quality. One might exploit this fact by using shallow circuits and set hard limit on training iterations. That would entail worse quality solutions on the subproblems and thus more possible nodes to evaluate. However since the subproblems get smaller and simpler, even shallow VQAs could solve them.

Since we build the tree of variable assignments, the algorithm guarantees optimality, even though not in polynomial time as the number of subproblems can be exponential. On the other hand, by solving the full problem at each node and reducing complexity at each level, our algorithm might find good quality solutions very early. This makes it an exciting candidate as a hybrid advice for classical solvers. Another advantage of this behavior is making quick decisions of a good enough quality, which is of great interest of industrial optimization.

And finally, even though our algorithm has many possibilities for improvement, our results prove that even in this early state it can produce measurable, good quality results with explainable, mathematical guarantees.

5.4 Implementation and integration

As our resources have been greatly limited, we are not able to provide extensive testing on real hardware, nor on scaled up problems. That is, we look forward to tackle problems from QOBLIB [48] with our approach with appropriate computational capabilities. We provided our results as numerical proofs, and provide the code as part of an open-source project at https://github.com/david-sipos/qcbb.

Declarations

- Funding: -
- Conflict of interest/Competing interests: The authors declare that they have no competing interests.
- Data availability: https://github.com/david-sipos/qcbb
- Author contribution: A.C. created the design of the algorithm. D.S. and B.G.-T. provided insights and guidance to the definition of the mathematical framework.
 A.C. and B.G.-T. formalized the idea. D.S. implemented, integrated and tested the algorithm. All authors have contributed to the manuscript.

References

- [1] Abbas A, Ambainis A, Augustino B, Bärtschi A, Buhrman H, Coffrin C, et al. Challenges and opportunities in quantum optimization. Nature Reviews Physics. 2024 Oct;6(12):718–735. https://doi.org/10.1038/s42254-024-00770-9.
- [2] Farhi E, Goldstone J, Gutmann S.: A Quantum Approximate Optimization Algorithm. arXiv. Available from: https://arxiv.org/abs/1411.4028.
- [3] Hadfield S, Wang Z, O'Gorman B, Rieffel EG, Venturelli D, Biswas R. From the Quantum Approximate Optimization Algorithm to a Quantum Alternating Operator Ansatz. Algorithms. 2019 Feb;12(2):34. https://doi.org/10.3390/a12020034.
- [4] Chalupnik M, Melo H, Alexeev Y, Galda A.: Augmenting QAOA Ansatz with Multiparameter Problem-Independent Layer. arXiv. Available from: https://arxiv.org/abs/2205.01192.

- [5] Motta M, Sun C, Tan ATK, O'Rourke MJ, Ye E, Minnich AJ, et al. Determining eigenstates and thermal states on a quantum computer using quantum imaginary time evolution. Nature Physics. 2019 Nov;16(2):205–210. https://doi.org/10. 1038/s41567-019-0704-4.
- [6] Soley MB, Bergold P, Batista VS. Iterative Power Algorithm for Global Optimization with Quantics Tensor Trains. Journal of Chemical Theory and Computation. 2021 May;17(6):3280–3291. https://doi.org/10.1021/acs.jctc.1c00292.
- [7] Gacon J, Nys J, Rossi R, Woerner S, Carleo G. Variational quantum time evolution without the quantum geometric tensor. Phys Rev Res. 2024 Feb;6:013143. https://doi.org/10.1103/PhysRevResearch.6.013143.
- [8] Kyaw TH, Soley MB, Allen B, Bergold P, Sun C, Batista VS, et al. Boosting quantum amplitude exponentially in variational quantum algorithms. Quantum Science and Technology. 2023 Oct;9(1):01LT01. https://doi.org/10.1088/ 2058-9565/acf4ba.
- [9] Andersen ED, Andersen KD. Presolving in linear programming. Mathematical Programming. 1995 Dec;71(2):221–245. https://doi.org/10.1007/bf01586000.
- [10] Achterberg T, Bixby RE, Gu Z, Rothberg E, Weninger D. Presolve Reductions in Mixed Integer Programming. INFORMS Journal on Computing. 2020 Apr;32(2):473–506. https://doi.org/10.1287/ijoc.2018.0857.
- [11] Kılınç Karzan F, Nemhauser GL, Savelsbergh MWP. Information-based branching schemes for binary linear mixed integer problems. Mathematical Programming Computation. 2009 Dec;1(4):249–293. https://doi.org/10.1007/ s12532-009-0009-1.
- [12] Achterberg T, Koch T, Martin A. Branching rules revisited. Operations Research Letters. 2005 Jan;33(1):42–54. https://doi.org/10.1016/j.orl.2004.04.002.
- [13] Berthold T, Lodi A, Salvagnin D. Primal Heuristics in Integer Programming. Cambridge University Press; 2025. Available from: http://dx.doi.org/10.1017/9781009574792.
- [14] Turner M, Koch T, Serrano F, Winkler M. Adaptive Cut Selection in Mixed-Integer Linear Programming. Open Journal of Mathematical Optimization. 2023 Jul;4:1–28. https://doi.org/10.5802/ojmo.25.
- [15] Zeng S, Zhang S, Li S, Wu F, Li XY.: Beyond Local Selection: Global Cut Selection for Enhanced Mixed-Integer Programming. arXiv. Available from: https://arxiv.org/abs/2503.15847.
- [16] Bravyi S, Kliesch A, Koenig R, Tang E. Obstacles to Variational Quantum Optimization from Symmetry Protection. Physical Review Letters. 2020 Dec;125(26).

- https://doi.org/10.1103/physrevlett.125.260505.
- [17] Bravyi S, Kliesch A, Koenig R, Tang E. Hybrid quantum-classical algorithms for approximate graph coloring. Quantum. 2022 Mar;6:678. https://doi.org/10.22331/q-2022-03-30-678.
- [18] Finžgar JR, Kerschbaumer A, Schuetz MJA, Mendl CB, Katzgraber HG. Quantum-Informed Recursive Optimization Algorithms. PRX Quantum. 2024 May;5(2). https://doi.org/10.1103/prxquantum.5.020327.
- [19] Zhang L, Lin X, Wang P, et al. Variational optimization for quantum problems using deep generative networks. Communications Physics. 2025;8:334. https://doi.org/10.1038/s42005-025-02261-4.
- [20] Egger DJ, Mareček J, Woerner S. Warm-starting quantum optimization. Quantum. 2021 Jun;5:479. https://doi.org/10.22331/q-2021-06-17-479.
- [21] Zhao Z, Fan L, Han Z. Hybrid Quantum Benders' Decomposition For Mixed-integer Linear Programming. In: 2022 IEEE Wireless Communications and Networking Conference (WCNC). IEEE; 2022. Available from: http://dx.doi.org/10.1109/WCNC51071.2022.9771632.
- [22] Montanaro A. Quantum speedup of branch-and-bound algorithms. Phys Rev Res. 2020 Jan;2:013056. https://doi.org/10.1103/PhysRevResearch.2.013056.
- [23] Chakrabarti S, Minssen P, Yalovetzky R, Pistoia M.: Universal Quantum Speedup for Branch-and-Bound, Branch-and-Cut, and Tree-Search Algorithms. arXiv. Available from: https://arxiv.org/abs/2210.03210.
- [24] Jarret M, Wan K. Improved quantum backtracking algorithms using effective resistance estimates. Phys Rev A. 2018 Feb;97:022337. https://doi.org/10.1103/ PhysRevA.97.022337.
- [25] Ambainis A, Kokainis M. Quantum algorithm for tree size estimation, with applications to backtracking and 2-player games. STOC 2017. New York, NY, USA: Association for Computing Machinery; 2017. p. 989–1002. Available from: https://doi.org/10.1145/3055399.3055444.
- [26] Czégel A, G Tóth B. A quantum constraint generation framework for binary linear programs. EPJ Quantum Technology. 2025 May;12(1). https://doi.org/10. 1140/epjqt/s40507-025-00364-z.
- [27] Karp RM. In: Reducibility among Combinatorial Problems. Springer US; 1972.
 p. 85–103. Available from: http://dx.doi.org/10.1007/978-1-4684-2001-2
 9.
- [28] Lucas A. Ising formulations of many NP problems. Frontiers in Physics. 2014;2. https://doi.org/10.3389/fphy.2014.00005.

- [29] Davis M, Putnam H. A Computing Procedure for Quantification Theory. Journal of the ACM. 1960 Jul;7(3):201–215. https://doi.org/10.1145/321033.321034.
- [30] Davis M, Logemann G, Loveland D. A machine program for theorem-proving. Communications of the ACM. 1962 Jul;5(7):394–397. https://doi.org/10.1145/368273.368557.
- [31] Goemans MX, Williamson DP. Improved approximation algorithms for maximum cut and satisfiability problems using semidefinite programming. Journal of the ACM. 1995 Nov;42(6):1115–1145. https://doi.org/10.1145/227683.227684.
- [32] Bharti K, Cervera-Lierta A, Kyaw TH, Haug T, Alperin-Lea S, Anand A, et al. Noisy intermediate-scale quantum algorithms. Rev Mod Phys. 2022 Feb;94:015004. https://doi.org/10.1103/RevModPhys.94.015004.
- [33] Chandarana P, Hegade NN, Paul K, Albarrán-Arriagada F, Solano E, del Campo A, et al. Digitized-counterdiabatic quantum approximate optimization algorithm. Physical Review Research. 2022 Feb;4(1). https://doi.org/10.1103/physrevresearch.4.013141.
- [34] Mundada PS, Barbosa A, Maity S, Wang Y, Merkh T, Stace TM, et al. Experimental Benchmarking of an Automated Deterministic Error-Suppression Workflow for Quantum Algorithms. Physical Review Applied. 2023 Aug;20(2). https://doi.org/10.1103/physrevapplied.20.024034.
- [35] Cai Z, Babbush R, Benjamin SC, Endo S, Huggins WJ, Li Y, et al. Quantum error mitigation. Reviews of Modern Physics. 2023 Dec;95(4). https://doi.org/10.1103/revmodphys.95.045005.
- [36] Zhu Y, Zhou Y, Cheng J, Jin Y, Li B, Niu S, et al. Compiler Optimizations for QAOA. In: Proceedings of the 43rd IEEE/ACM International Conference on Computer-Aided Design. ICCAD '24. ACM; 2024. p. 1–7. Available from: http://dx.doi.org/10.1145/3676536.3697127.
- [37] Sipos D, Czégel A, Tóth BG.: Variational Quantum Optimization Benchmark Suite for Airline Crew Pairing and More. arXiv. Available from: https://arxiv. org/abs/2504.11899.
- [38] Powell MJD. In: A Direct Search Optimization Method That Models the Objective and Constraint Functions by Linear Interpolation. Springer Netherlands; 1994. p. 51–67. Available from: http://dx.doi.org/10.1007/978-94-015-8330-5_4.
- [39] Berthold T. Measuring the impact of primal heuristics. Operations Research Letters. 2013 Nov;41(6):611–614. https://doi.org/10.1016/j.orl.2013.08.007.
- [40] Alessandroni E, Ramos-Calderer S, Roth I, Traversi E, Aolita L. Alleviating the quantum Big-M problem. npj Quantum Information. 2025 Jul;11(1). https://doi.org/10.1016/jul.2025.1016.

- //doi.org/10.1038/s41534-025-01067-0.
- [41] Rehfeldt D, Koch T, Shinano Y. Faster exact solution of sparse Max-Cut and QUBO problems. Mathematical Programming Computation. 2023 Apr;15(3):445–470. https://doi.org/10.1007/s12532-023-00236-6.
- [42] The Quadratic Unconstrained Binary Optimization Problem: Theory, Algorithms, and Applications. Springer International Publishing; 2022. Available from: http://dx.doi.org/10.1007/978-3-031-04520-2.
- [43] Cheng L, Chen YQ, Zhang SX, Zhang S. Quantum approximate optimization via learning-based adaptive optimization. Communications Physics. 2024 Mar;7(1). https://doi.org/10.1038/s42005-024-01577-x.
- [44] Zhang Z, Paredes R, Sundar B, Quiroga D, Kyrillidis A, Duenas-Osorio L, et al. Grover-QAOA for 3-SAT: quadratic speedup, fair-sampling, and parameter clustering. Quantum Science and Technology. 2024 Nov;10(1):015022. https://doi.org/10.1088/2058-9565/ad895c.
- [45] Bakó B, Glos A, Salehi O, Zimborás Z. Prog-QAOA: Framework for resource-efficient quantum optimization through classical programs. Quantum. 2025 Mar;9:1663. https://doi.org/10.22331/q-2025-03-20-1663.
- [46] Weidenfeller J, Valor LC, Gacon J, Tornow C, Bello L, Woerner S, et al. Scaling of the quantum approximate optimization algorithm on superconducting qubit based hardware. Quantum. 2022 Dec;6:870. https://doi.org/10.22331/q-2022-12-07-870.
- [47] Tuan Hai V, Tan Viet N, Urbaneja J, Vu Linh N, Nguyen Tran L, Bin Ho L. Multi-target quantum compilation algorithm. Machine Learning: Science and Technology. 2024 Dec;5(4):045057. https://doi.org/10.1088/2632-2153/ad9705.
- [48] Koch T, Neira DEB, Chen Y, Cortiana G, Egger DJ, Heese R, et al.: Quantum Optimization Benchmark Library The Intractable Decathlon. arXiv. Available from: https://arxiv.org/abs/2504.03832.
- [49] Barahona F, Jünger M, Reinelt G. Experiments in quadratic 0–1 programming. Mathematical Programming. 1989 May;44(1–3):127–137. https://doi.org/10.1007/bf01587084.
- [50] Garey MR, Johnson DS. Computers and Intractability: A Guide to the Theory of NP-Completeness. San Francisco: W. H. Freeman; 1979.
- [51] Papadimitriou CH, Yannakakis M. Optimization, approximation, and complexity classes. Journal of Computer and System Sciences. 1991 Dec;43(3):425–440. https://doi.org/10.1016/0022-0000(91)90023-x.

A Binary Linear Program to Ising Hamiltonian

We show the calculations how we transform the binary linear program to Ising Hamiltonian. This is a very common conversion, however we use some of the elements in the main text, therefore we show this derivation explicitly.

A.1 Conversion

As a first step we create a QUBO form from (MP) with moving the constraints to the objective as

$$Ax = b \longmapsto (Ax - b)^{T} (Ax - b) \tag{23}$$

$$= (x^T A^T A x - 2(Ax)^T b + b^T b) (24)$$

$$= x^{T} (A^{T} A)x - 2(Ax)^{T} b + b^{T} b$$
(25)

so the problem becomes, with a sufficiently large penalty factor, M

$$\min \left\{ x^T (MA^T A) x + c^T x - 2M (Ax)^T b + M b^T b \mid x \in \{0, 1\}^n \right\}. \tag{26}$$

Now we change the domain from $x \in \{0,1\}$ to $\sigma \in \{-1,1\}$ by substituting $x = \frac{\sigma + 1}{2}$,

$$H(x) = x^{T} (MA^{T}A)x + (c^{T} - 2Mb^{T}A)x + Mb^{T}b$$
(27)

$$= \frac{\sigma^T + \mathbf{1}^T}{2} (MA^T A) \frac{\sigma + \mathbf{1}}{2} + (c^T - 2Mb^T A) \frac{\sigma + \mathbf{1}}{2} + Mb^T b$$
 (28)

$$= \frac{1}{4}M\sigma^{T}(A^{T}A)\sigma + \frac{1}{2}M\mathbf{1}^{T}(A^{T}A)\sigma + \frac{1}{4}M\mathbf{1}^{T}(A^{T}A)\mathbf{1}$$
 (29)

$$+\frac{1}{2}c^{T}\sigma + \frac{1}{2}\mathbf{1}^{T}c - Mb^{T}A\sigma - Mb^{T}A\mathbf{1} + Mb^{T}b$$
 (30)

$$= \frac{1}{4}M\sigma^{T}(A^{T}A)\sigma + \frac{1}{2}\left(c^{T} - 2Mb^{T}A + M\mathbf{1}^{T}(A^{T}A)\right)\sigma \tag{31}$$

$$+\frac{1}{4}M\mathbf{1}^{T}(A^{T}A)\mathbf{1} + \frac{1}{2}\mathbf{1}^{T}c - Mb^{T}A\mathbf{1} + Mb^{T}b$$
(32)

and then the problem resolves to

$$H(\sigma) = -\sum_{i < j} J_{ij}\sigma_i\sigma_j - \mu \sum_i h_i\sigma_i + C,$$
(33)

where

$$J = -\frac{1}{4}MA^{T}A\tag{34}$$

and

$$h = c^{T} - 2Mb^{T}A + M\mathbf{1}^{T}(A^{T}A)$$
(35)

with

$$\mu = -\frac{1}{2}.\tag{36}$$

The constant term C does not affect the procedure and thus can be put aside during optimization and add back after. The constant is

$$C = \frac{1}{4}M\mathbf{1}^{T}(A^{T}A)\mathbf{1} + \frac{1}{2}\mathbf{1}^{T}c - Mb^{T}A\mathbf{1} + Mb^{T}b.$$
 (37)

Here we arrived at an Ising Hamiltonian $H(\sigma)$ with σ noting its spin configuration.

A.2 Big M value

Big M should be a sufficiently large constant. For any feasible x and any infeasible x',

$$c^{T}x < c^{T}x' + M(Ax' - b)^{T}(Ax' - b).$$
 (38)

must hold. In [26] we have derived a big M value, for the numerical precision κ needed for A and b,

$$M = \frac{1}{\kappa} \sum_{i} |c_{i}| \ge \frac{\max_{x,x'} c^{T} (x - x')}{\min_{x'} (Ax' - b)^{T} (Ax' - b)} \ge \max_{x,x'} \frac{c^{T} (x - x')}{(Ax' - b)^{T} (Ax' - b)}.$$
 (39)

B Bounding calculations

Here we describe the exact calculation behind the bounding step. We calculate a lower bound using an approximate solution to the Maximum Cut problem.

B.1 Maximum Cut problem

This problem is defined on an undirected graph G = (V, E) with weights on its edges $w_{uv} \in \mathbb{R} \setminus \{0\}, (u, v) \in E, u, v \in V$. We denote edges between sets $U, W \subset V$ by $(u, v) \in E(U, W)$, where $u \in U, v \in W$ and $(u, v) \in E$. Now, a cut $g(S), S \subseteq V$ is a bipartition of the vertices, where the value of the cut is given by the sum of weights between the partitions:

$$g(S) = \sum_{(u,v)\in E(S,V\setminus S)} w_{uv}.$$
 (40)

The problem is to find the cut with the greatest value, i.e.

$$z^* = \max_{S \subseteq V} g(S) = \max_{S \subseteq V} \sum_{(u,v) \in E(S,V \setminus S)} w_{uv}. \tag{41}$$

B.2 Reduction of $H(\sigma)$ to Maximum Cut

Recall that H is an Ising Hamiltonian operator over n spins $\sigma \in \{1, -1\}^n$, and has the form of

$$H(\sigma) = -\sum_{i < j} J_{ij}\sigma_i\sigma_j - \mu \sum_j h_i\sigma_i.$$
 (42)

We derive the following reduction to the Maximum Cut problem, based on the reduction from [49]. Given a Hamiltonian with J and h as on (42), we define the following

graph: $V = \{0, 1, ..., n\}, E = \{(0, i) \mid i \in V \setminus \{0\}, h_i \neq 0\} \cup \{(i, j) \mid i, j \in V \setminus \{0\}, J_{ij} \neq 0, i < j\}$ with edge weights $w_{ij} = J_{ij} \ \forall (i, j) \in E, i \neq 0$, and $w_{0i} = \mu h_i \ \forall i \in V \setminus \{0\}$, where $h_i \neq 0$.

The domain of the variables is still $\{-1,1\}$. Interpreting it in the domain of the binary Maximum Cut problem, for each assignment of the variables σ_i , let us organize them to two disjoint sets of vertices of the graph. Since the problem is symmetric, we can choose vertex 0 to be part of any of the sets. Then, defining $V^+ = \{i \in V \mid \sigma_i = 1\} \cup \{0\}$ and $V^- = \{i \in V \mid \sigma_i = -1\}$, by construction we get the following, equivalent minimization problem:

$$\min H(\sigma) = \min \sum_{(i,j) \in E(V^+, V^+)} w_{ij} + \sum_{(i,j) \in E(V^-, V^-)} w_{ij} - \sum_{(i,j) \in E(V^+, V^-)} w_{ij}$$
(43)

which is equivalent to

$$\min \sum_{(i,j)\in E} w_{ij} - 2 \sum_{(i,j)\in E(V^+,V^-)} w_{ij}. \tag{44}$$

Now if we take a look on $\sum_{(i,j)\in E(V^+,V^-)} w_{ij}$, this is exactly the objective value from

the formulation of the Maximum Cut, where $V^+ = S$ and which we denoted above by $g(V^+)$. If we take the optimal solution, $z^* = \max_{V^+ \subseteq V} g(V^+)$, we arrive at

$$\min H(\sigma) = -2z^* + W,\tag{45}$$

where

$$W = \sum_{(i,j)\in E} w_{ij} = \sum_{i< j} J_{ij} + \mu \sum_{i} h_{i}.$$
 (46)

B.3 Approximate solution to Maximum Cut

The Maximum Cut problem is NP-hard [50], its decision version is NP-complete [27]. It is also APX-hard [51], meaning there is no efficient ϵ -approximation algorithm exists unless P=NP. However, there is an efficient, semidefinite programming (SDP) relaxation based randomized algorithm by Goemans and Williamson [31] with a worst-case average approximation ratio $\alpha = 0.87856$. That means, for an undirected, positively weighted graph G, with maximal cut value z^* and the cut value from the Goemans-Williamson algorithm z_{GW} , we get

$$\alpha z^* \le z_{GW} \le z^*,\tag{47}$$

so that we can use z_{GW} for bound calculation.

B.4 The lower bound

Here we provide the bound calculation as well as a lower bound to the bound itself. Since we have negative edge weights as well in the graph, we need the following Theorem 3.2.1 from [31]. For the graph G = (V, E), encoding the problem, we have defined W as the sum of the edge weights,

$$W = \sum_{(i,j)\in E} w_{ij},\tag{48}$$

We now extend that definition to graphs with negative edge weights by defining the total negative edge weights,

$$W^{-} = \sum_{(i,j)\in E: w_{ij} < 0} w_{ij}, \tag{49}$$

and we will use the already introduced notation of $\alpha = 0.87856$ for the average approximation ratio of the Goemans-Williamson algorithm. In this section we derive a lower bound to min $H(\sigma)$, of the form of (MH) (and (RH)), using these notations.

Theorem 1 ([31], Theorem 3.2.1.). Let z_{GW} the expected value of the maximum cut on G from the algorithm, and z^* the maximal cut value, then

$$z_{GW} - W^- \ge \alpha \left(z^* - W^- \right).$$

Theorem 2. Given an Ising Hamiltonian subproblem min $H(\sigma)$ of the form of (MH), and its reduction to Maximum Cut on graph G. Let z_{GW} denote the solution from the Goemans-Williamson algorithm on G. Then,

$$LB_{GW}(H(\sigma)) = -\frac{2}{\alpha}z_{GW} + \left(\frac{2}{\alpha} - 2\right)W^{-} + W$$

is a lower bound to min $H(\sigma)$, i.e.

$$LB_{GW}(H(\sigma)) \le \min H(\sigma)$$
.

Proof. According to Theorem 1, in our case, where negative edge weights are also considered, we can derive that

$$z^* \le \frac{1}{\alpha} z_{GW} - \left(\frac{1}{\alpha} - 1\right) W^-. \tag{50}$$

Let us consider the reduction in Section B.2 from an Ising Hamiltonian H to a Maximum Cut problem on graph G. Using the Goemans-Williamson algorithm to find the maximum cut on G and by combining (45) and (50), we get

$$\min H(\sigma) = -2z^* + W \tag{51}$$

$$\geq -2\left(\frac{1}{\alpha}z_{GW} - \left(\frac{1}{\alpha} - 1\right)W^{-}\right) + W \tag{52}$$

$$= -\frac{2}{\alpha}z_{GW} + \left(\frac{2}{\alpha} - 2\right)W^{-} + W \tag{53}$$

Thus, a valid lower bound is

$$LB_{GW}(H(\sigma)) = -\frac{2}{\alpha} z_{GW} + \left(\frac{2}{\alpha} - 2\right) W^{-} + W. \tag{54}$$

Theorem 3. The lower bound $LB_{GW}(H(\sigma))$ cannot be worse then

$$LB = \frac{1}{\alpha} \min H(\sigma) - \left(\frac{1-\alpha}{\alpha}\right) \left(W - 2W^{-}\right)$$

calculated from the optimum, that is,

$$LB \le LB_{GW}(H(\sigma)) \le \min H(\sigma).$$

Proof. The error of the approximation, i.e. the difference between the optimal solution value $\min H(\sigma)$ and $LB_{GW}(H(\sigma))$ is given by

$$\Delta_{approx} = \min H(\sigma) - LB_{GW}(H(\sigma)) \tag{55}$$

$$= -2z^* + W - \left(-\frac{2}{\alpha}z_{GW} + \left(\frac{2}{\alpha} - 2\right)W^- + W\right)$$
 (56)

$$= -2z^* + \frac{2}{\alpha}z_{GW} - \left(\frac{2}{\alpha} - 2\right)W^-.$$
 (57)

Now this shows an interesting behavior. Since $z_{GW} \leq z^*$, given any H, the largest difference from the optimal solution value so the worst bound occurs when $z_{GW} = z^*$. The better result the approximation algorithm produces, the worst bound we obtain:

$$\max \Delta_{approx} = \max_{z_{GW}} \left(-2z^* + \frac{2}{\alpha} z_{GW} - \left(\frac{2}{\alpha} - 2\right) W^- \right)$$
 (58)

$$= \left(\left(\frac{2}{\alpha} - 2 \right) z^* - \left(\frac{2}{\alpha} - 2 \right) W^- \right) = \left(\frac{2}{\alpha} - 2 \right) \left(z^* - W^- \right). \tag{59}$$

Therefore the bound $LB_{GW}(H(\sigma))$ is in the worst case, due to (54) and (59),

$$\min H(\sigma) - \left(\frac{2}{\alpha} - 2\right) \left(z^* - W^-\right) \le LB_{GW}(H(\sigma)) \le \min H(\sigma) \tag{60}$$

The worst bound, in terms of the elements of the Ising Hamiltonian H is, since $z^* = -\frac{1}{2} \left(\left(\min H(\sigma) \right) - W \right)$,

$$LB = \min H(\sigma) - \left(\frac{2}{\alpha} - 2\right) \left(z^* - W^-\right) \tag{61}$$

$$= \min H(\sigma) + \frac{1}{2} \left(\frac{2}{\alpha} - 2 \right) \left(\min H(\sigma) - W + 2W^{-} \right)$$
 (62)

$$= \frac{1}{\alpha} \min H(\sigma) + \left(\frac{1}{\alpha} - 1\right) \left(-W + 2W^{-}\right), \tag{63}$$

what had to be shown.

Remark 1. The result of Theorem 3 can be written in terms of the Hamiltonian, i.e.

$$LB = \frac{1}{\alpha} \min H(\sigma) - \left(\frac{1}{\alpha} - 1\right) \left(\sum_{i < j} |J_{ij}| + \mu \sum_{i} |h_i|\right).$$
 (64)

This is due to the construction of the graph, and its weights W (48). Similarly to W^- (49), we can define the sum of positive edge weights as W^+ , so that $W = W^+ + W^-$. From that, we have the following simple expansion:

$$W - 2W^{-} = W^{+} - W^{-} \tag{65}$$

$$= \sum_{i < j} |J_{ij}| + \mu \sum_{i} |h_i|. \tag{66}$$

C Infeasibility proof using M

Based on the bound calculation above, we can derive a condition that is sufficient to prove a subproblem infeasible.

Statement 4. When $LB_{GW}(\hat{H}) + \hat{C} \geq M$, the subproblem, encoded in \hat{H} , is infeasible.

Proof. It is by the design of the calculations of M and the lower bound.

By the construction in (39), M dominates all feasible solution values, meaning that for each feasible solution \hat{x} , and its value $\hat{c}^T\hat{x} = \hat{H} + \hat{C}$, it is true that

$$\hat{c}^T \hat{x} < M. \tag{67}$$

As for the lower bound, $LB_{GW}(\hat{H})$ is a lower bound to $\min_{\hat{x}} \hat{c}^T \hat{x} - \hat{C} = \min_{\hat{\sigma}} \hat{H}$. That means, for any feasible solution \hat{x} , it holds that

$$\hat{c}^T \hat{x} \ge L B_{GW}(\hat{H}) + \hat{C}. \tag{68}$$

Let us suppose that there exist a feasible solution \hat{x} for which $LB_{GW}(\hat{H}) + \hat{C} \geq M$. Then by (39) and (68) we have

$$LB_{GW}(\hat{H}) + \hat{C} \ge M > \hat{c}^T \hat{x} \ge LB_{GW}(\hat{H}) + \hat{C}.$$
 (69)

Combining the two gives a contradiction, therefore there is no feasible solution for the subproblem, if its lower bound is at least M.

D Number of many-body terms over the levels

Statement 5. The number of many-body terms does not increase at each sub-problem creation step. Formally, following the notation of Section 3.2, the number of non-zero elements above the main diagonal in the child node \tilde{J} is less than or equal to their number in the parent node \hat{J} .

Proof. Since $J = -\frac{1}{4}MA^TA$, we need to take a look at \hat{A} and \tilde{A} . We get a zero in A^TA if either two columns of A have a zero inner product or at least one of the columns is a zero vector. We choose variables that has the greatest conflict values. We can exclude the latter, all-zero columns, since by construction, we would never choose a variable to fix that does not appear in any constraints.

For the pairwise orthogonal columns, we can only guarantee that their number do not decrease by more than $\hat{n}-1$. Let us suppose that we remove column k from \hat{A} . If that column had zero inner product with each of the other columns, we would end up removing $\hat{n}-1$ zeros from above the main diagonal of \hat{A} when constructing \tilde{A} . Since the difference between the above-diagonal elements of \hat{J} and \tilde{J} are exactly this set of entries, we did not remove any non-zeros from \hat{J} .

Any other cases would include removing non-zeros from above the main diagonal, and thus remove many-body terms from the operator. That is, because the removal operation does not affect any other elements but the ones in the column k, which we remove.

In the latter case, the variables are completely independent from each other. That case could on one hand, slow our solution process down. On the other hand it is an opportunity for decomposition of the problem.

E Convergence of the bounds

Here we show that both the solutions that we find and the lower bound, calculated by the Goemans-Williamson algorithm converges to the optimal solution value of (MP). This is a criterion to use the primal-dual integral [39] to measure the solution process quality, and also to provide a comparison to classical solvers.

The statement is a consequence of the construction of the algorithm. At any point, the frontier of the tree includes both the current best solution (incumbent, upper bound) and the current global lower bound. We also know the exact relation between the bounds, as the incumbent must be greater or equal to the lower bound, see Appendix B.

Since at each subproblem creation, we fix at least one variable and remove it from further optimization, the bound calculation becomes more precise. At the same time, the lower bound itself is also at least equal to lower bound of the problem in the parent node by definition in (19), and thus in the root. Formally, using the notation of Section 3.2.3,

$$LB(\hat{H}) + \hat{C} < LB(\tilde{H}) + \tilde{C}. \tag{70}$$

When there are no more free variable left in the subproblem, either the two local bounds meet or we prove the subproblem infeasible. If the bounds meet, that is formally due to there is nothing to approximate to get a lower bound, and thus it becomes 0 + fixed values. That is exactly the local upper bound. On a side note we can end up pruning the sub-tree completely, which does not affect global convergence since we do not lose optimal solutions by pruning the sub-tree.

Putting the pieces together, on each path from the root node, the complete problem, to a leaf node, a subproblem with no variables, we either have a proof of infeasibility, non-improvement or a proof of local optimum.

We can evaluate all the nodes on all such paths from the root to any of the end nodes, infeasible, pruned or leaf. Due to the removal of at least one variable on each level, the number of nodes to evaluate is $2^n - 1$. In the end, we can enumerate all the leaf nodes, and look for the best solution as that will provide a global optimum.

Of course computationally this does not help, but proves that for each problem we can obtain either a proof of infeasibility, a proof of an existing better solution, or a proof of optimality.

F Further numerical results and algorithm characteristics

Here we show results obtained on a variety of problem instances, similar to those shown in Section 4. We've opted to showcase a range of problem instances that range from easier to more difficult as judged by the number node evaluations required for the bounds to converge.

As in Figure 3, Figure 6 showcases the convergence of the upper bound, given by the incumbent solution at a given node, and the lower bound, calculated using the approximate solution of the corresponding MaxCut instance. Possible use of these bounds is as a termination criterion, or as a quality measure of the process of the solver. In our testing, it seems that for easier to solve instances the gap closes suddenly as the optimal solution is found, likely as a result of variable propagation. In more difficult instances, we see the gap closing in sooner than the last couple of iterations, for such problems the node-selection and variable-selection processes can greatly impact the performance of the algorithm.

Similar to Figure 4, in Figure 7 we show the fraction of many-body terms present, compared to (MH), as the tree is being explored as a blue line with circular markers. In some instances, we can see that due to order of evaluations, and thus the plot itself, not following the tree structure, occasional increases are present as the algorithm explore nodes higher up in the tree or those where variable propagation resulted in fewer variables being removed.

As with the instance in Figure 5, in Figure 8 we continue to see a clear advantage attributable to the subproblem reduction step as the expected cost associated with the quantum state drops (shown in blue) as we switch to solving smaller and smaller subproblems. With plain QAOA the improvements plateau out fairly early and while it can achieve lower expected cost with fewer queries, in the long run our approach achieves lower expected cost, which can suggest a high probability of sampling favorable variable assignments. Here we can still observe the potential impact the specifics of the VQA used can have. In many cases we see only a slow improvement attributable to the VQA optimization process, with larger intermittent drops likely the effect of subproblem reductions. Note that expected costs can be greatly skewed by sampling infeasible solutions, which have very high costs due to penalty terms introduced as part of the QUBO formulation.

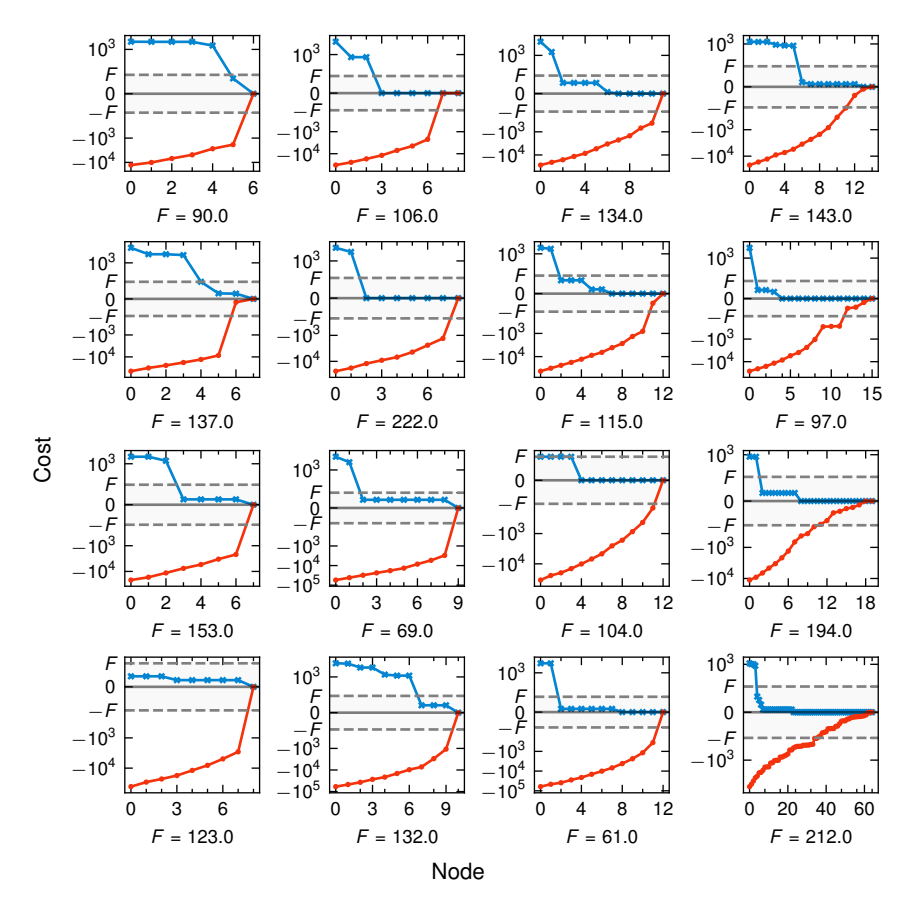


Figure 6 Convergence of bounds for 16 problem instances. Similar to Figure 3, a blue line with x-shaped markers shows the upper bound (cost of incumbent solution) as a function of the number of nodes evaluated. The red line with circular markers shows the lower bound as the function of the number of nodes evaluated. A solid black line marks the optimum, aligned to 0, with dashed black lines representing the cost F of the worst feasible solution, with its value shown under each subfigure. Between the dashed lines the y axis is scaled linearly while outside the dashed line a logarithmic scale is used.

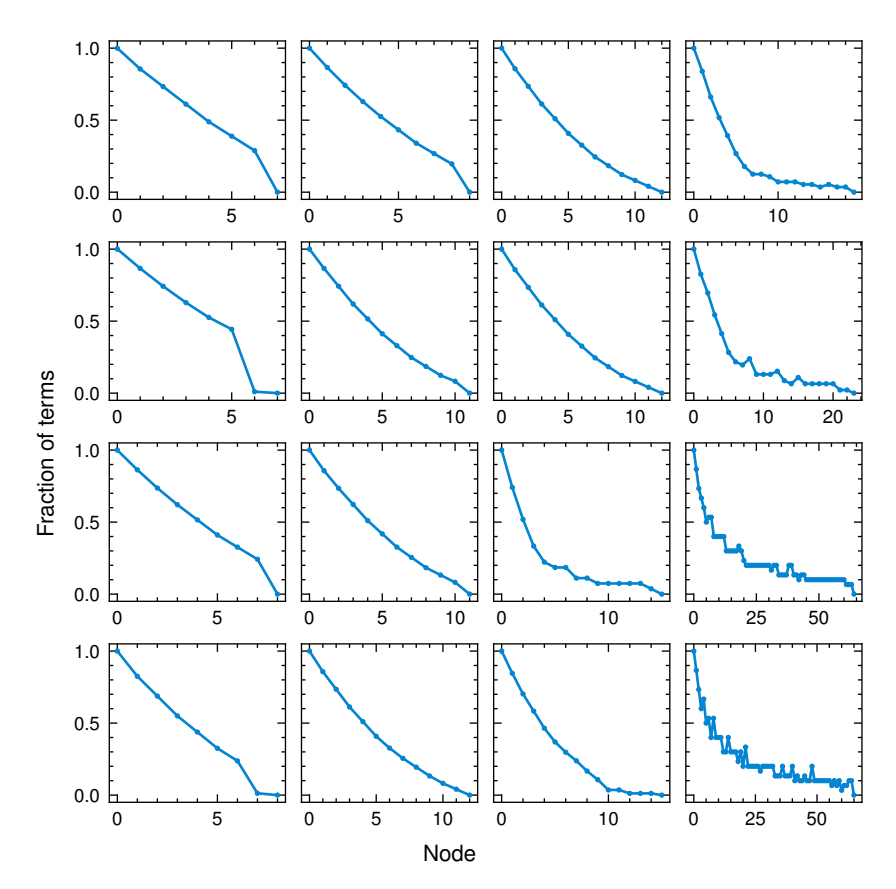


Figure 7 Fraction of many-body terms for 16 problem instances. Similar to Figure 4, a blue line with circular markers shows the fraction of many-body terms remaining (compared to (MH)) as a function of nodes evaluated.

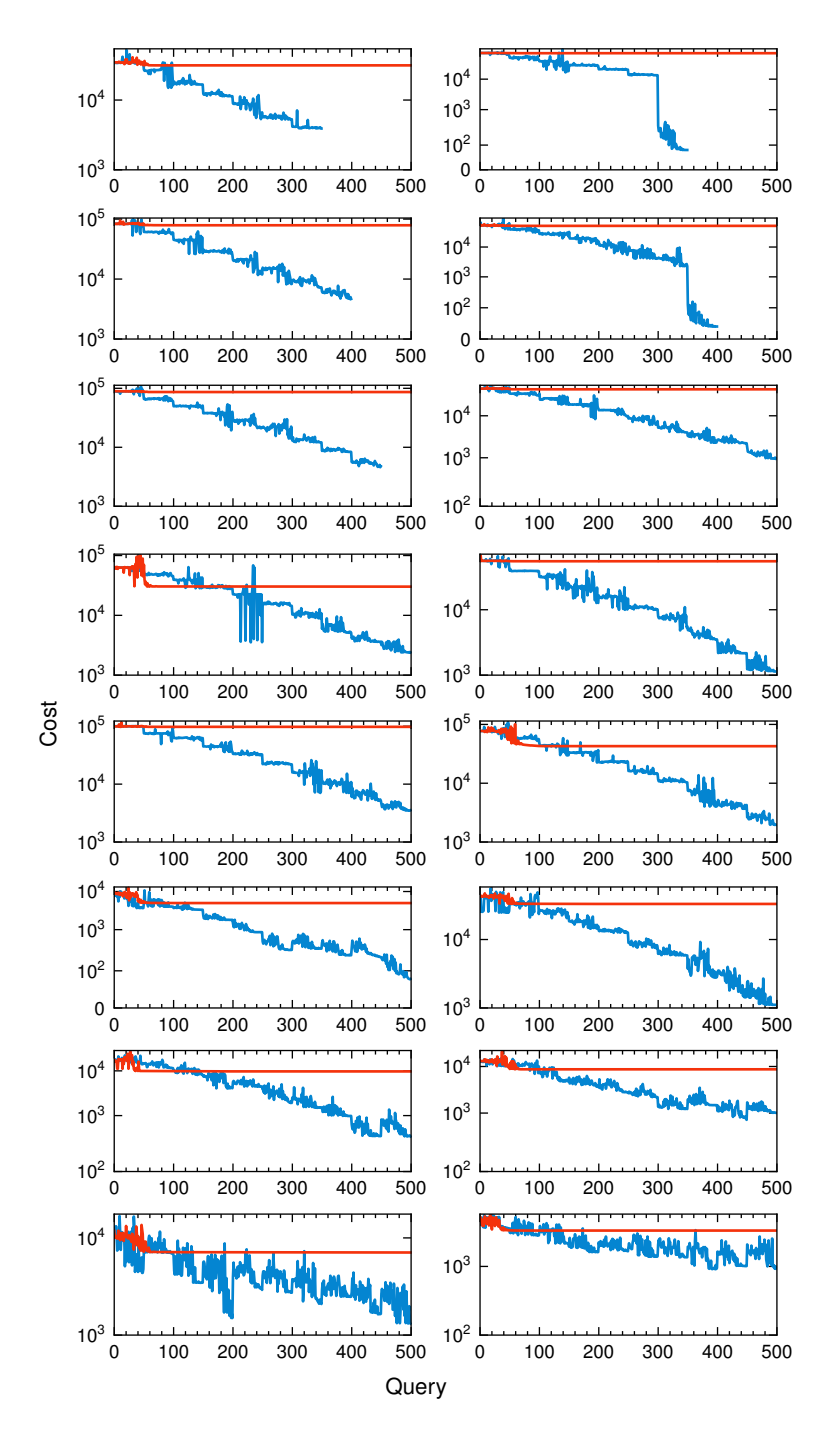


Figure 8 Comparison of branch and bound with plain QAOA for 16 problem instances. The plots show the expected cost associated with the quantum state, as a function of queries made to a quantum simulator, as it evolves during the execution of the VQA in each node. Values on the y axis show distance from the optimum. For each instance, plotted in blue, we use the branch and bound approach proposed in this work with a limit of 50 iterations per node. For the red line, only QAOA is used. 31